Decoupled Control System for Cascaded H-Bridge Multilevel Converter Based STATCOM

***Abstract*— In conventional control systems for Cascaded H-Bridge (CHB) multilevel converter based STATCOM the action of individual voltage controllers which balance the capacitors voltages can alter the output of the cluster voltage controller and the current controller due to a coupling effect. In this paper, first, the conditions that eliminate this coupling effect are derived and then a control system that enforces the derived decoupling conditions is proposed. It is also shown, that additional advantage of the proposed decoupled control system is that it enables linearization of the cluster voltage control loop. Experimental studies on a single-phase 7-level STATCOM demonstrate effectiveness of the proposed decoupled control system in improving the transient performance of the STATCOM.**

***Index Terms*— Cascaded H-Bridge, decoupled control system, multilevel converter, STATCOM, voltage balancing.**

I. Introduction

THE Cascaded H-Bridge (CHB) converter is one of the popular types of multilevel converters. Compared to other widely used multilevel converter topologies such as the neutral-point-clamped or diode-clamped and the flying capacitor topologies, the CHB converter topology has lower number of components [1]. Furthermore, its modular structure and high number of redundant switching states are attractive features of this topology [2]. On the other hand, the requirement of multiple isolated DC sources is considered its main drawback [2]. However, in applications such as reactive power compensation, solar photovoltaic power generation and rectification, where the isolated DC sources are readily available the previously mentioned requirement can be an advantage [3]-[11].

In reactive power compensators maintaining the balance between the DC voltages of the H-bridges is a challenge, because the DC voltages are not regulated by an external rectifier circuit or a battery. The methods proposed in the literature to balance the voltages of the DC capacitors in CHB converters can be classified into two different categories.

In the first category, the switching redundancies are exploited to balance the voltages [12]-[20]. For instance, in [12] the proposed modification of the model predictive control scheme for a CHB based STATCOM exploits the switching redundancy to balance the voltages of the capacitors, minimize the switching losses, and track the sinusoidal current reference simultaneously. The idea proposed in [12], was further improved in [13], by introducing a new voltage balancing model that considered not only the position of the capacitor voltage, when sorted in comparison to others, but also the difference between each capacitor voltage and its target reference. Therefore, as the model included more information about the system, a more optimal solution was expected. However, by increasing the number of levels, the required computations to find the optimal switching states increased. Furthermore, the switching frequency of different H-bridge bridges was different. A generalized voltage balancing technique for a CHB rectifier using a hybrid modulation technique was presented in [14]. A low frequency control loop was added to achieve the voltage balance among the H-bridges and manage the operating state of each bridge. An improved version of this work presented in [15] further increased the stable operating region of the system. In this case, each H-bridge operated with a different switching frequency which is not desirable. However, none of these papers have discussed the effect of balancing action on the cluster voltage controller.

One of the disadvantages of the methods belonging to the first category is that a central switching controller is required for the system and the PWM generator is not modular which makes the system extension to higher voltage levels difficult. Moreover, a system based on the central switching module depends on high-bandwidth communications to transmit time critical PWM signals [21]. Furthermore, by increasing the number of converter levels the number of redundant states grows which makes the balancing mechanism complicated.

Voltage balancing methods in the second category use modular PWM techniques such as the Phase Shift PWM (PS-PWM) along with internal individual voltage controllers for each H-bridge [22]-[27]. For example, in [22] three different control architectures to control the capacitor voltages for a five-level converter were compared. It was shown that only one configuration (one cluster voltage controller for the overall voltage, one controller for each of the individual DC voltages, one current controller) worked well for all reference voltages and loads. Therefore, in a general case an N-level converter requires (N-1) individual capacitor voltage controllers to balance the voltages of the DC capacitors and one cluster voltage controller to generate the reference for the active component of the grid current. However, the paper did not discuss the coupling effects among these controllers. In [23], the active power requirement of each H-bridge was controlled using a separate PI controller. The AC voltage reference of corresponding cell was modified in accordance to the individual voltage controller. In [24], similar control architecture was proposed in which a PI controller was assigned to regulate the voltage of each capacitor. Using small signal detailed modeling it was shown that the gain of the transfer function was time variant. This time variant part was removed by introducing an extra compensator in the loop of the individual voltage controllers. However, none of these papers discussed the coupling effect among the controllers.

The manuscript is submitted for review on 29 Aug 2014, revised on 5 Feb 2015 and 15 Apr 2015.

Compared to the control methods in the first category, the methods in the second category have the advantage of using symmetrical switching techniques that maintain equal switching frequency for all of the H-bridges. Furthermore, there is no need for algorithms to select optimal switching combination to reach the control goals. However, having a separate controller for each H-bridge makes the control system complicated especially for higher number of levels and this can be considered a disadvantage. Furthermore, the individual voltage control loop is coupled to the rest of the control system which makes the design of the overall control system complicated [28]. In [25], the dynamics of the individual voltage controllers were intentionally slowed down in order to avoid its interactions with the cluster voltage controller. However, the coupling was not removed and its effect was attenuated by reducing the bandwidth of the voltage balancing control system. The coupling effect of the voltage balancing to the current controller was identified and compensated for the control system proposed in [28]. However, no attempt was made to identify and eliminate the coupling effect to the cluster voltage controller. In [29], capacitor voltage balancing was achieved by active voltage superposition in which an active component was superimposed on the reference voltage of each H-bridge to change its absorbed power. A comprehensive study based on vector analysis was provided to determine the stability and regulation capacity of the balancing strategy. Furthermore, it was shown that the superimposed voltages will not disturb the total output voltage of the inverter. Hence, similar to [28], decoupling from the current controller was achieved. However, the coupling effect of the balancing strategy to the cluster voltage controller was not provided.

The novelty of this paper compared to previous works is that the conditions that eliminate the coupling effect between the voltage balancing controller and the rest of the control system are identified and then a control system that imposes the derived decoupling conditions is proposed. The decoupled control system proposed in this paper belongs to the second category. However, as compared to the previously proposed control systems, it has the advantage of completely decoupling the individual capacitor voltage controllers from the cluster voltage controller and the current controller. The decoupling is achieved by (i) controlling the sum of the squares of the capacitor voltages in the cluster voltage controller to be constant and (ii) by requiring the sum of the changes applied by the individual voltage controllers to the H-bridges output voltages to be zero. Additional advantage of the proposed decoupled control system is that it linearizes the cluster voltage control loop. Presented experimental results demonstrate effectiveness of the proposed decoupled control system in improving the transient performance of a single-phase 7-level STATCOM.

The rest of this paper is organized as follows; Section II derives a CHB converter-based STATCOM model. Derivation of the decoupling conditions and the proposed decoupled control system is introduced in Sections III and IV. Experimental results are provided in Section V. Finally, conclusions are summarized in Section VI.

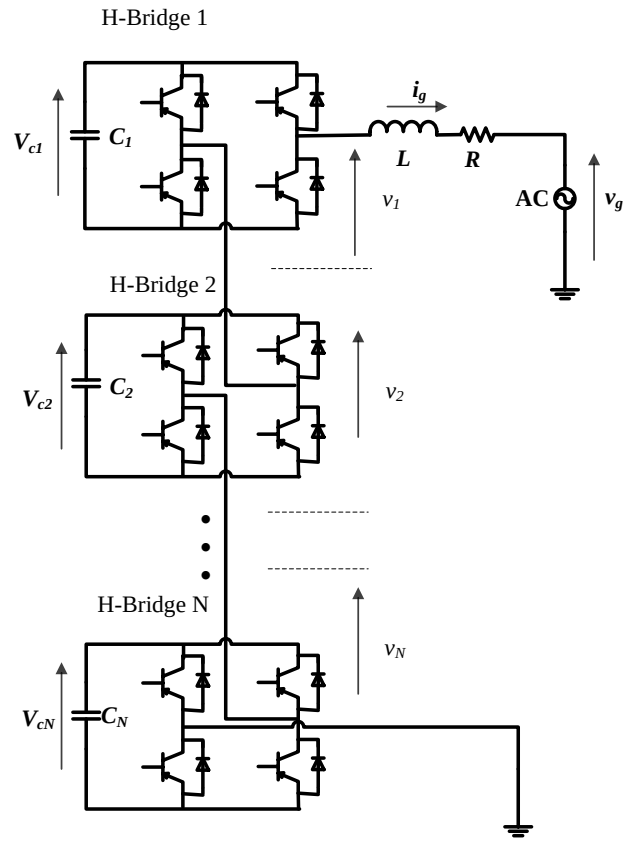

Fig. 1. A general configuration of a (2*N+1*)-level single-phase CHB converter-based STATCOM

II. CHB Converter Based STATCOM Model

A general configuration of a (2*N+1*)-level single-phase CHB converter-based STATCOM is shown in Fig. 1. Applying KVL to the AC side yields

$$\sum_{j=1}^{N} v_j - v_g - Ri_g - L\frac{di_g}{dt} = 0 \tag{1}$$

where v_j is the output voltage generated by the jth H-bridge, L represents the inductance of the filtering inductor and R is its series resistance. v_g and i_g are the grid voltage and current respectively.

On the other hand, applying KCL to N DC nodes at the DC side gives

$$I_{C-j} + C\frac{dV_{cj}}{dt} = 0 \quad , \quad (j = 1, \cdots, N). \tag{2}$$

In which C represents the capacitance of the capacitors ($C=C_1=C_2=\ldots=C_N$) and V_{cj} is the voltage across the individual capacitors. I_{C-j} represents the current flowing into the jth capacitor. Assuming that the losses are negligible, the input power on the AC side is equal to the output power on the DC side. Hence,

$$I_{C-j} = \frac{v_j}{V_{cj}} i_g \quad , \quad (j = 1, \cdots, N). \tag{3}$$

Substituting $I_{c\text{-}j}$ from (3) in (2) yields,

$$\frac{v_j}{V_{cj}} i_g + C\frac{dV_{cj}}{dt} = 0 \quad , \quad (j = 1, \ldots, N) \tag{4}$$

(1) and (4) model dynamic behavior of the CHB converter-based STATCOM. (1) governs the grid current dynamics controlled by the total generated output voltage of the converter. On the other hand, (4) is used to balance the individual capacitor voltage of each H-bridge by modifying the active component of its generated output voltage.

III. Decoupling Conditions

The individual capacitor voltage controller tries to balance the capacitors voltages by controlling the amount of active power flown into the capacitor of each H-Bridge. Hence, this controller introduces an additional term to the AC voltage reference of each H-Bridge to control distribution of the active power among the H-Bridges. Therefore, it is desirable that the action of this controller does not interfere with the grid current which is regulated by different controller. In the following steps the conditions that have to be met in order to decouple the individual capacitor voltage controller from the rest of the control system are derived.

Due to the action of the capacitor voltage balancing (1) and (4) can be rewritten as

$$\sum_{j=1}^{N}(v_j + \Delta v_j) - v_g - R(i_g + \Delta i_g) - L\frac{d(i_g + \Delta i_g)}{dt} = 0 \tag{5}$$

$$\frac{v_j + \Delta v_j}{V_{cj}}(i_g + \Delta i_g) + C\frac{dV_{cj}}{dt} = 0 \quad , \quad (j = 1, \ldots, N) \tag{6}$$

where Δv_j represents the voltage change due to the action of the individual capacitor voltage controller and Δi_g is the perturbation in the grid current due to Δv_j.

To ensure that the individual voltage controller does not interfere with the rest of the control system, Δi_g must be zero. Therefore, assuming $\Delta i_g = 0$, (5) can be rewritten as

$$\sum_{j=1}^{N}(v_j + \Delta v_j) - v_g - Ri_g - L\frac{di_g}{dt} = 0. \tag{7}$$

Hence, from (1) and (7), the first condition for having a decoupled control system is,

$$\sum_{j=1}^{N}\Delta v_j = 0. \tag{8}$$

Similarly, assuming $\Delta i_g = 0$ in (6) yields,

$$\frac{v_j + \Delta v_j}{V_{cj}} i_g + C\frac{dV_{cj}}{dt} = 0 \quad , \quad (j = 1, \ldots, N). \tag{9}$$

In (9), the change in the voltage of the capacitor is caused by ($v_j\ i_g$) and ($\Delta v_j\ i_g$). By separating the effect of each term, (9) can be rewritten as,

$$\frac{v_j + \Delta v_j}{V_{cj}} i_g + C\frac{\partial V_{cj}}{\partial(v_j i_g)}\frac{d(v_j i_g)}{dt} + C\frac{\partial V_{cj}}{\partial(\Delta v_j i_g)}\frac{d(\Delta v_j i_g)}{dt} = 0 \quad , \quad (j = 1, \ldots, N). \tag{10}$$

Using (4), (10) can be rewritten as

$$\frac{\Delta v_j}{V_{cj}} i_g + C\frac{\partial V_{cj}}{\partial(\Delta v_j i_g)}\frac{d(\Delta v_j i_g)}{dt} = 0 \quad , \quad (j = 1, \ldots, N). \tag{11}$$

Rearranging (11) gives,

$$i_g \Delta v_j = -CV_{cj}\frac{\partial V_{cj}}{\partial(\Delta v_j i_g)}\frac{d(\Delta v_j i_g)}{dt} \quad , \quad (j = 1, \ldots, N). \tag{12}$$

Summing all equations in (12) gives,

$$\sum_{j=1}^{N} V_{cj}\frac{\partial V_{cj}}{\partial(\Delta v_j i_g)}\frac{d(\Delta v_j i_g)}{dt} = \frac{-i_g}{C}\sum_{j=1}^{N}\Delta v_j. \tag{13}$$

Now, using (8), (13) becomes

$$\sum_{j=1}^{N} V_{cj}\frac{\partial V_{cj}}{\partial(\Delta v_j i_g)}\frac{d(\Delta v_j i_g)}{dt} = 0. \tag{14}$$

Taking the integral of (14) yields

$$\sum_{j=1}^{N} V_{cj}^2 = \sum_{j=1}^{N} K_j. \tag{15}$$

In (15), K_j is an arbitrary constant which can be set to a desired reference value, e.g., $V^2_{cj\text{-}ref}$. Therefore,

$$\sum_{j=1}^{N} V_{cj}^2 = \sum_{j=1}^{N} V_{cj-ref}^2 \tag{16}$$

which is the second condition for having a decoupled control system.

As all of the steps to derive (8) and (16) from (7) and (9) are reversible, it can be concluded that (8) and (16) are the two sufficient and necessary conditions that have to be met in order to decouple the control system. Condition (8) necessitates that the individual voltage controllers should not alter the total AC voltage of the converter and hence guarantees decoupling from the current controller. Condition (16) shows that the cluster voltage controller should regulate

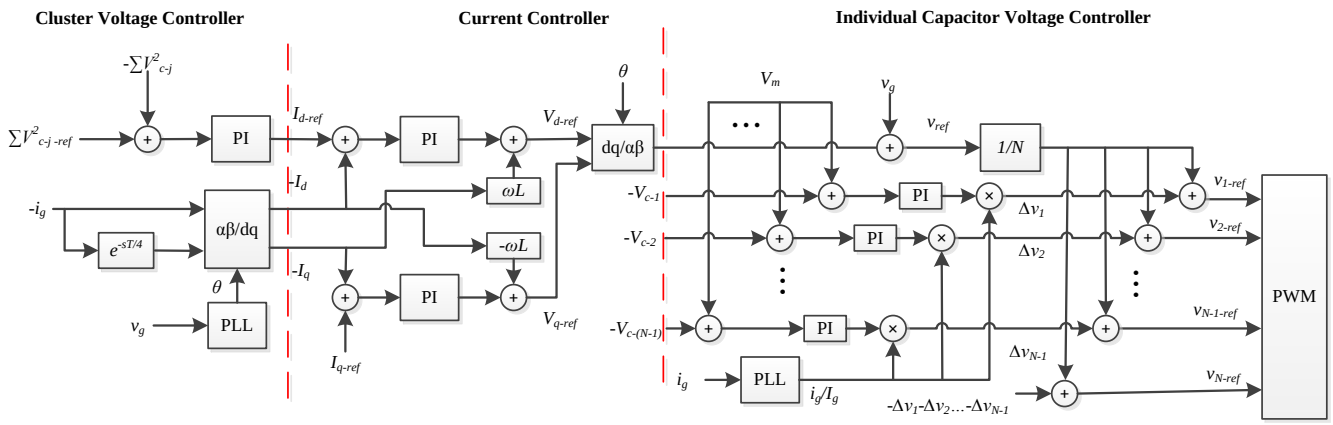

Fig. 2. CHB based STATCOM control system composed of three subsystems, a cluster voltage controller, a current controller, and individual capacitor voltage controllers with voltage balancing.

the sum of the squares of the voltages and is equivalent to regulating the total energy stored in the capacitors. Hence, if (16) is met then the individual capacitor voltages balancing method can exchange the power between the H-bridges without interfering with the cluster voltage controller.

It is worth mentioning that violation of (8) will alter the reference voltage generated by the current controller and hence it will directly affect the current, while violation of (16) will produce perturbation in the output of cluster voltage controller and hence it will have indirect effect on the current.

IV. Decoupled Control System

The block diagram of the proposed decoupled control system that is composed of a cluster voltage controller, a current controller and an individual voltage controller for each H-bridge is shown in Fig. 2. The active power is controlled by the *d*-axis component of the grid current. Hence, the reference *d*-axis current component $I_{d\text{-}ref}$ is generated by the cluster voltage control loop controlled by a PI controller. On the other hand, the reference *q*-axis current, $I_{q\text{-}ref}$, which determines the reactive power of the converter can be generated by a secondary controller such as a grid voltage controller. The resulting reference grid current is then regulated using PI controllers in the *d-q* reference frame. The required orthogonal *α-β* components of the current for transformation are generated by introducing a quarter of the grid current period time delay to the original current [30].

A. Individual Capacitor Voltage Controllers and Voltage Balancing

Unlike in a conventional two-level converter, the capacitor voltage control system of the CHB converters requires a balancing mechanism in order to regulate the individual capacitors voltages. In total, there are (*N-1*) PI controllers to generate Δv_1 to Δv_{N-1}. The function of the individual voltage controllers is not to push the capacitor voltages towards their required reference values as this is the function of cluster voltage controller. The individual voltage controllers only try to keep the voltages balanced. Therefore, the reference value for all individual voltage PI controllers is

$$V_m = \frac{\sum_{j=1}^{N} V_{cj}}{N} = \frac{V_d}{N}. \tag{17}$$

Each individual voltage controller adds an incremental voltage, Δv_j, to the AC voltage reference (v_{ref}/N) of each H-Bridge. The function of this incremental voltage term is to exchange the active power between the H-Bridges and therefore it is in phase with the grid current. Hence, Δv_j is positive for the H-Bridges with higher capacitor voltage in order to discharge them and negative for the ones with lower capacitor voltage in order to charge them. The incremental voltage Δv_N for the last *N*-th H-bridge is determined considering the condition (8) as

$$\Delta v_N = -\sum_{j=1}^{N-1} \Delta v_j. \tag{18}$$

Hence, the total reference AC voltage for each H-Bridge is

$$v_{j-ref} = \frac{v_{ref}}{N} + \Delta v_j \quad , \quad (j = 1, \ldots, N) \tag{19}$$

where v_{ref} is the inverter AC reference voltage generated by the current controller.

B. Cluster Voltage Controller

In the proposed control system the cluster voltage controller uses the sum of squares of the capacitors voltages instead of the sum of the voltages in order to satisfy the condition (16). Other than a requirement for decoupling, using the square of the voltages linearizes the cluster voltage control loop which in turn simplifies the cluster voltage controller design. To elaborate further, considering only the DC value of the active power, a simplified block diagram for a conventional control system is shown in Fig. 3. The transfer function G_V of the conventional control system shown in Fig. 3 is

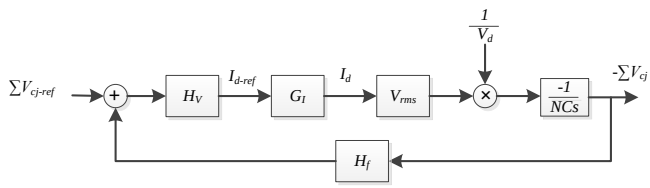

Fig. 3. Conventional cluster voltage control system

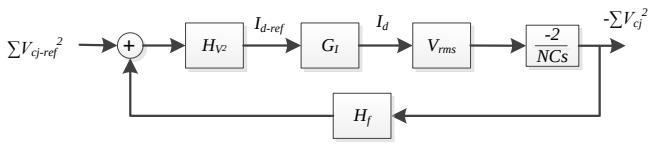

Fig. 4. Proposed cluster voltage control system

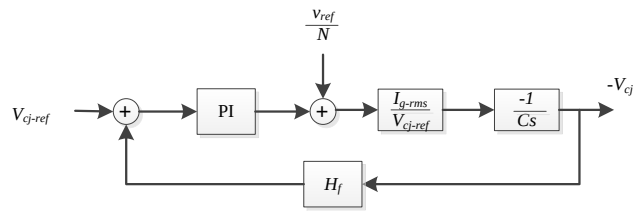

Fig. 5. Individual capacitor voltage control loop

$$G_V = \frac{\sum V_{cj}}{\sum V_{cj-ref}} = \frac{V_{rms} G_I H_V}{NCV_d s + V_{rms} G_I H_V H_f} \tag{20}$$

where G_I is the transfer function of the current controller, H_V is the transfer function of the PI cluster voltage controller of the conventional coupled system, and V_{rms} is the RMS value of the grid voltage. (20) is valid only if the voltage V_d is assumed to be constant and set to the nominal operating point, i.e., $V_d = \sum V_{cj\text{-}ref}$. Therefore, if the voltage V_d deviates from its nominal operating point, the system dynamics will change and affect the performance of the control loop.

However, by applying the condition (16) the control system in Fig. 3 is transformed into a linear system as shown in Fig. 4. Now, the transfer function becomes

$$G_{V^2} = \frac{\sum V_{cj}^2}{\sum V_{cj-ref}^2} = \frac{2V_{rms} G_I H_{V^2}}{NCs + V_{rms} G_I H_{V^2} H_f} \tag{21}$$

which is valid at any operating point. In (21), H_{V^2} represents the transfer function of the PI cluster voltage controller for the decoupled system. The linearity is especially important during the transients or in applications such as photovoltaic systems where the voltage changes in a wide range due to the action of the maximum power point tracking scheme and the small signal linearization of the system is no longer valid.

V. Simulations

The parameters of the selected CHB based STATCOM system used for simulations are given in Table I. Detailed design of the converter is provided in [9]. The simulations are carried out in MATLAB/Simulink environment.

The design of the controllers was carried out using Interactive mode, Robust response time, PID tuning method in the Matlab control system designer tool. For the current controller the constraint of the bandwidth, f_i, is $f_i \leq 0.2 f_s$. Hence, the design objectives for the current controller were f_i=100 Hz and 60^0 phase margin.

The design of the PI cluster voltage controller and the individual capacitor PI voltage controllers was carried out based on the control loop shown in Figs. 4 and 5 respectively. The cluster voltage controller bandwidth, f_v, is limited by two constraints; $f_v \leq 0.1 f_i$, and $f_v \leq 0.2 f_g$. Hence, the design objectives for the cluster voltage controller were f_v=10 Hz and 60^0 phase margin. The cutoff frequency of the feedback filter was 50 Hz to remove the unwanted low frequency ripple on the capacitor voltages. The same criteria were applied to design the individual voltage controllers.

The open loop Bode diagrams of the proposed and the conventional cluster voltage controllers are shown in Fig. 6. As stated before, characteristics of the proposed controller do not change for different operating points, whereas, for the conventional one, the controller moves towards instability as

TABLE I
Parameters of the Simulated System

Symbol	Quantity	Values
$V_{g\text{-}rms}$	Grid voltage *rms* value	6 kV
C	H-bridge DC capacitance	9.2×10^{-3} F
L	Filter inductance	3.5 mH
$V_{c\text{-}ref}$	Capacitor reference voltage	1.9 kV
f_s	Switching frequency	500 Hz
f_g	Grid frequency	50 Hz
S	Converter nominal power	3 MVAr
R	Filter inductor series resistance	0.2 Ω
f_v	Bandwidth of the voltage controller	10 Hz
f_i	Bandwidth of the current controller	100 Hz
N	Number of H-bridges	5

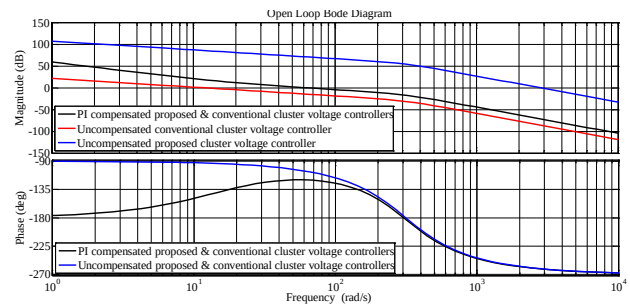

Fig. 6. Open loop Bode diagrams of the proposed and the conventional cluster voltage controllers.

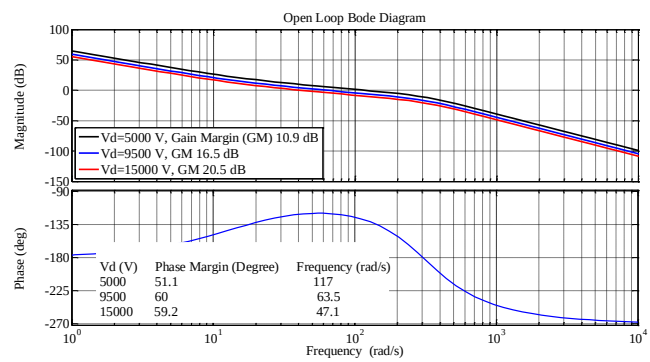

Fig. 7. Effect of V_d on the open loop Bode diagram of the conventional cluster voltage controller.

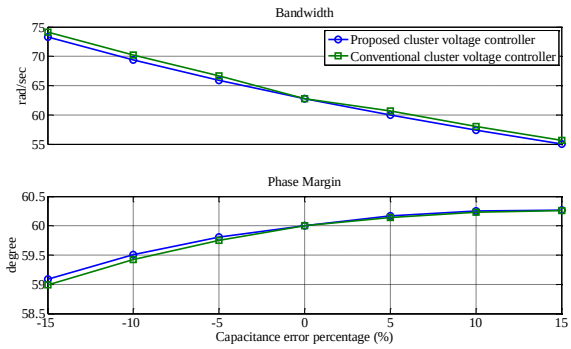

Fig. 8. Sensitivity of the proposed and the conventional cluster voltage controllers to the capacitance.

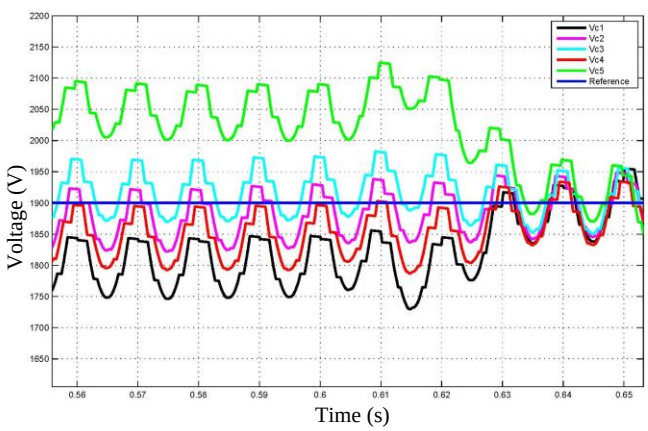

Fig. 9. Capacitors' voltages before and after activation of the voltage balancing.

V_d decreases as shown in Fig. 7.

The sensitivity of the proposed and conventional cluster voltage controller to the capacitance of the capacitors is shown in Fig. 8. From these results it can be concluded that the sensitivity for both controllers remains the same.

Capability of the proposed control scheme to regulate the capacitor voltages is confirmed for two different cases.

In the first case, initially, the balancing mechanism is switched off and the system is exchanging the rated reactive power with the grid. Then, at time t=0.5s the balancing mechanism is switched on. As it can be seen from Fig. 9, the proposed balancing mechanism successfully returned the voltages to their reference values. The output of the cluster voltage controller for the proposed decoupled control system that uses the square of the voltages and for the conventional control system is shown in Fig. 10. As it can be seen in the case of the proposed control system the action of balancing does not disturb this signal whereas, for the conventional one, it underwent a transient.

In the second case, a step change in the reference reactive power is studied. Here, the reactive current reference is suddenly changed from full reactive to full capacitive at time t=0.8 s. As it can be seen in Fig. 11, the proposed controller is able to regulate the capacitors voltages even during the transients.

VI. Experimental Results

A 7-level single-phase CHB converter based STATCOM

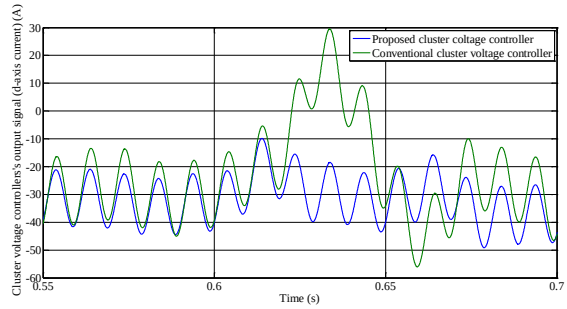

Fig. 10. Comparison of the proposed and the conventional cluster voltage controller output signals.

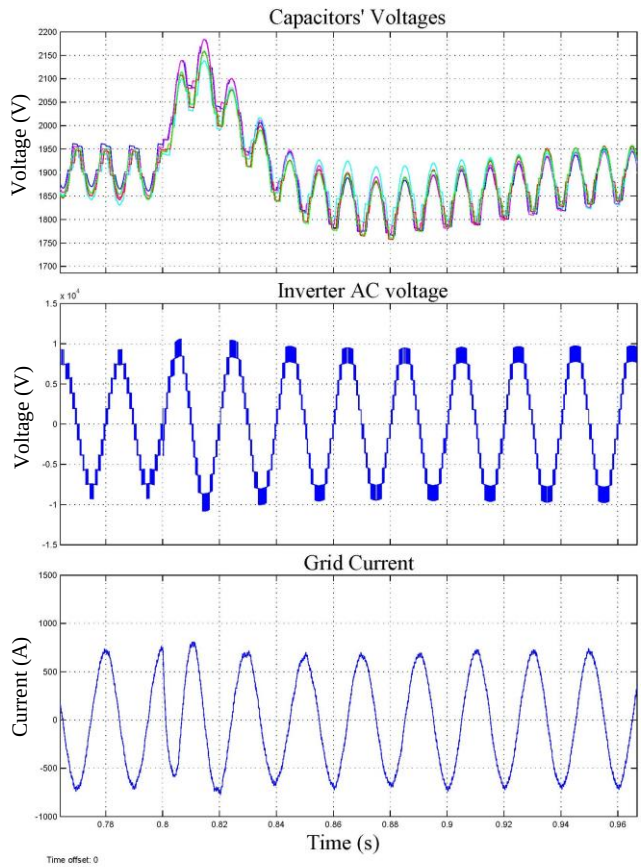

Fig. 11. Simulation results illustrating the grid current, the inverter AC voltage and the capacitors voltages when the reactive current reference is suddenly changed from fully capacitive to fully inductive at t_0

was used to experimentally verify the proposed decoupling conditions. A photograph of the experimental test bench is shown in Fig. 12. 240 V grid voltage was reduced to 110 V using an isolation transformer. Three POWEREX PP75B060 single-phase H-bridge converters were connected in series to form a 7-level CHB converter. The phase-shifted SPWM was implemented using the dSPACE DS5203 FPGA module. A feed-forward compensation technique was also implemented to mitigate the adverse effect of the second order capacitors' voltages ripples on the AC current, in which, the online sampled capacitor voltages were used to calculate the per-unit reference signal for the SPWM module [31]. All control systems were implemented using the dSPACE DS1006

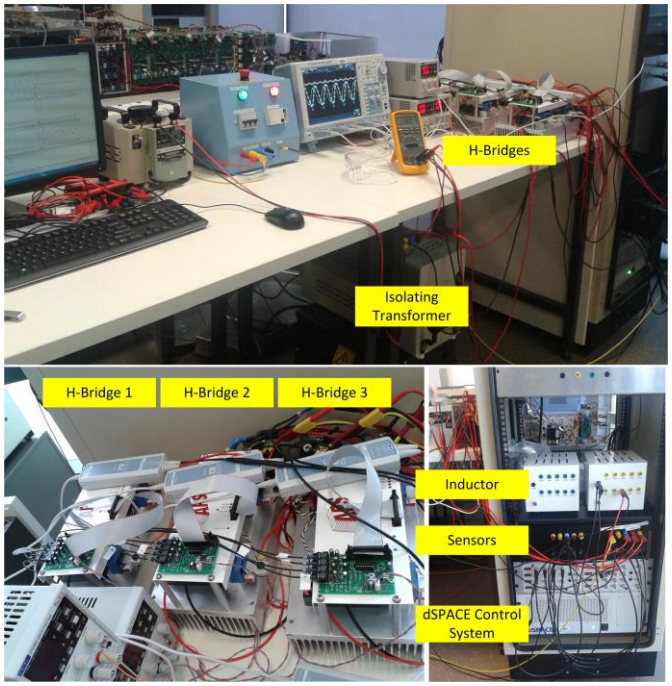

Fig. 12. Experimental setup of a single-phase 7-level CHB converter based STATCOM

processor board. The feedback signals were fed back to the processor board using the dSPACE DS2004 ADC module. The parameters of the experimental setup are provided in Table II.

Firstly, effectiveness of the proposed decoupling conditions is studied by monitoring the cluster voltage controller output and the grid current during the transients. Then, the linearity of the decoupled control system is verified. Finally, results verifying operation of the STATCOM are provided to demonstrate the viability of the proposed decoupled control system.

A. Coupled Versus Decoupled Control System

In this section the effect of each decoupling condition is investigated individually. The following four cases are analyzed.

Case I: both condition (8) and (16) are satisfied (proposed decoupled control system).

Case II: condition (8) is satisfied and (16) is violated.

Case III: condition (8) is violated and (16) is satisfied.

Case IV: both condition (8) and (16) are violated.

Initially, the individual voltage controllers are switched off and the system is exchanging the rated reactive power with the grid. Then, at t≈0.06s the individual voltage controllers are switched on.

In Cases III and IV, in order to violate the condition (8), Δv_N is set to zero instead of calculating it from (18). In Cases II and IV, condition (16) is violated by using the sum of the voltages instead of the sum of the squares of voltages in the cluster voltage controller. The cluster voltage controller loop has a bandwidth of 63 rad/s and the required sum of the capacitor voltages is 240 V. In all of the cases individual voltage controllers and the current controller parameters are the same.

TABLE II
PARAMETERS OF THE EXPERIMENTAL SETUP

Symbol	Quantity	Values
$V_{g\text{-}rms}$	Grid voltage *rms* value	110 V
C	H-bridge DC capacitance	3.3×10^{-3} F
L	Filter inductance	8 mH
$V_{c\text{-}ref}$	Capacitor reference voltage	80 V
f_s	Switching frequency	2 kHz
f_g	Grid frequency	50 Hz
S	Converter nominal power	1100 VA
R	Filter inductor series resistance	0.5 Ω
f_F	Cut-off frequency of the capacitor voltage filter	25 Hz
ξ	Damping factor of the capacitor voltage filter	0.707
f_v	Bandwidth of the voltage controller	10 Hz
f_i	Bandwidth of the current controller	400 Hz
$K_{V\text{-}i}$	Integral gain of the cluster voltage controller	4.8×10^{-3}
$K_{V\text{-}p}$	Proportional gain of the cluster voltage controller	5.3×10^{-3}
$K_{i\text{-}i}$	Integral gain of the current controller	875
$K_{i\text{-}p}$	Proportional gain of the current controller	20
$K_{b\text{-}i}$	Integral gain of the individual voltage controller	2.6
$K_{b\text{-}p}$	Proportional gain of the individual voltage controller	2.6
N	Number of H-bridges	3

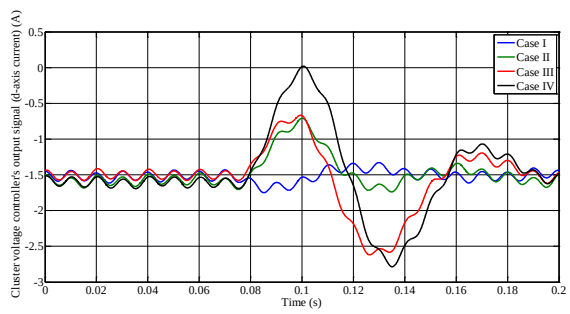

Fig. 13. Experimental results illustrating effect of the decoupling conditions (8) and (16) on the cluster voltage controller output, Case I: both condition (8) and (16) are satisfied, Case II: condition (8) is satisfied and (16) is violated, Case III: condition (8) is violated and (16) is satisfied, Case IV: both condition (8) and (16) are violated.

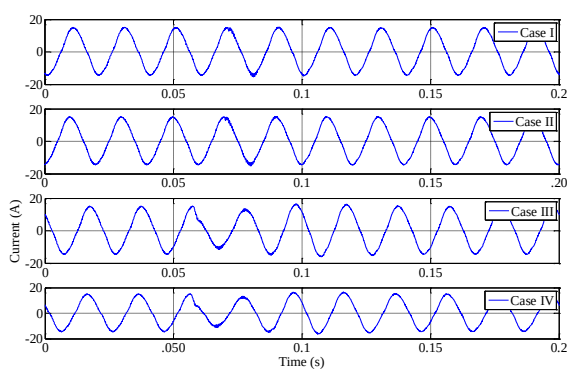

Fig. 14. Experimental results illustrating effect of the decoupling conditions (8) and (16) on the grid current.

The outputs of the cluster voltage controller for all four cases are shown in Fig. 13. The grid currents are shown in Fig. 14. As it can be seen in Fig. 13, for the decoupled control system (Case I) the output of the cluster voltage controller

remains almost unchanged while for the coupled one it is disturbed. The disturbance in Case III is caused by transients in the grid current due to the term added to the current controller output by the individual voltage controllers. Therefore, the magnitude of the disturbance depends on the amplitude of this additional term. In Case II, the magnitude of the disturbance is related to the energy mismatch between the unbalanced capacitors voltages and the balanced ones. Hence, the magnitude of the disturbance depends on the capacitance and the DC voltage magnitude. The two factors do not necessarily act in the same direction and in some cases they might cancel out each other's effect. However, in this study the effects are combined since the disturbance is the largest when both the decoupling conditions are violated (Case IV).

As for the grid current, violation of (8) results in significant disturbances in the grid current while the effect of violation of (16) is not as significant, as shown in Fig. 14. This result is predictable because (8) has a direct effect on the output current while (16) can only affect the output current indirectly through $I_{d\text{-}ref}$ which is usually negligible compared to the total current. For instance in this case the reactive current reference is 10 A while the disturbance in $I_{d\text{-}ref}$ caused by violation of (16) is only about 0.8 A as shown in Fig. 13 (Case II). As expected, the best results are achieved when both decoupling conditions are satisfied.

B. Demonstration of Cluster Voltage Control Loop Linearity

Fig. 15 compares performance of conventional and proposed cluster voltage control system in response to a step change in the reference voltage. As it can be seen, when using the proposed decoupled (linear) control system the dynamics of the voltage remain the same while for the conventional one the response becomes slower as the reference voltage increases.

C. STATCOM Operation

In this section, performance of the proposed control system in the most common operating scenario of a STATCOM, i.e. a step change in the reference of the reactive power is studied. Here, the reactive current reference is suddenly changed from full capacitive to full inductive at t_0. The grid current, the grid voltage, and the capacitors voltages during this test are shown in Fig. 16. As it can be seen, the proposed control system is able to follow the reactive power reference quickly and regulate the voltages of the capacitors during the transients.

Fig. 17, shows the effectiveness of the individual capacitor voltage controllers in balancing the capacitors voltages. In this experiment the STATCOM is exchanging its nominal reactive power with the grid. The waveforms show the capacitors voltages and the grid voltage and current before and after the activation of the individual voltage controllers at t_0. As it can be seen the controller restored the balance to the capacitors voltages without producing any disturbances in the grid current which confirms correct operation of the decoupled control system.

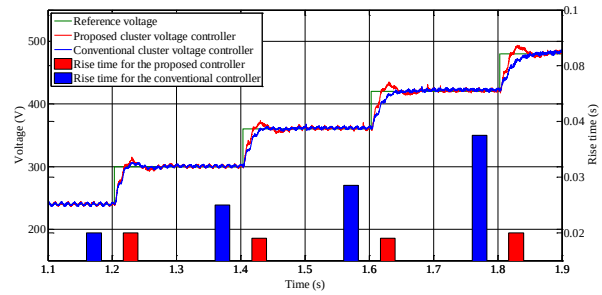

Fig. 15. Comparison of performance of conventional and proposed cluster voltage control system in response to a step change in the reference voltage.

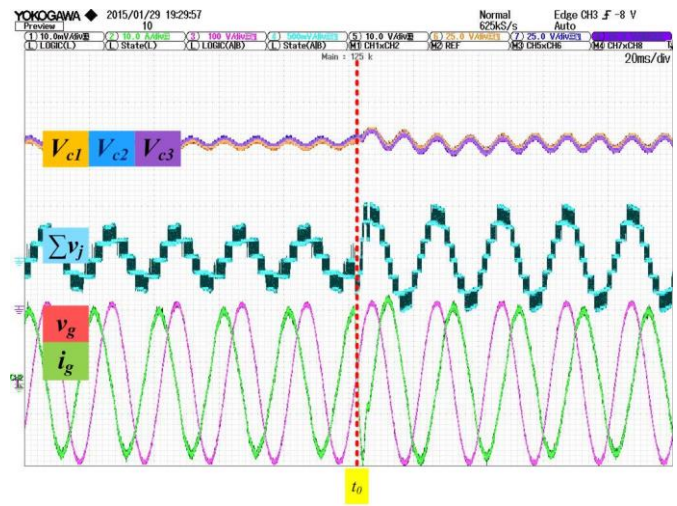

Fig. 16. Experimental results illustrating the grid current, the grid voltage and the capacitors voltages when the reactive current reference is suddenly changed from fully capacitive to fully inductive at t_0

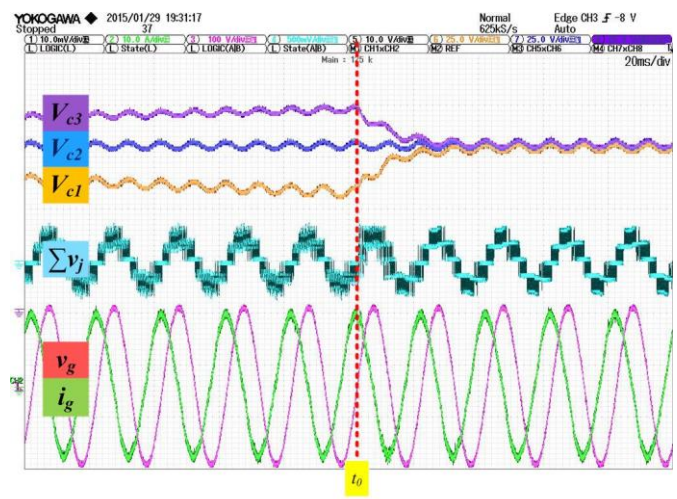

Fig. 17. Experimental results illustrating the grid current, the grid voltage and the capacitors voltages before and after activation of individual voltage controllers at t_0

D. Effect of inaccuracy in the inductance L of the filtering inductor on the control system

In this section the effect of inaccuracy in the inductance of the filtering inductor L on the control system is investigated. In this paper L is assumed to be constant, which is a good assumption, because the current rating of the inductor used in the experiments is 20 A. Therefore, the operating point will

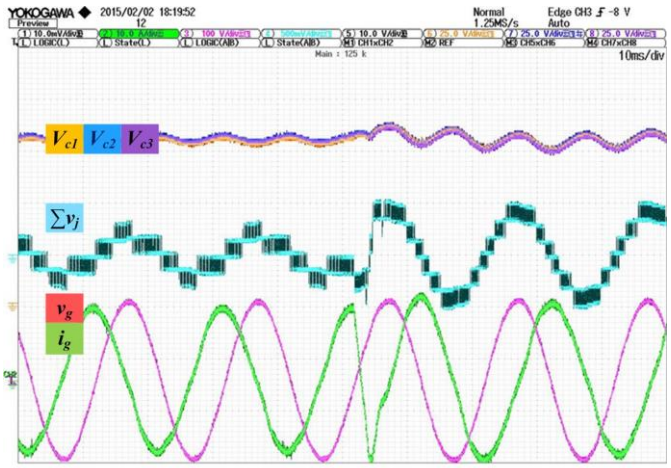

Fig. 18. Control system performance during sudden reactive power change with +25% increase in *L*.

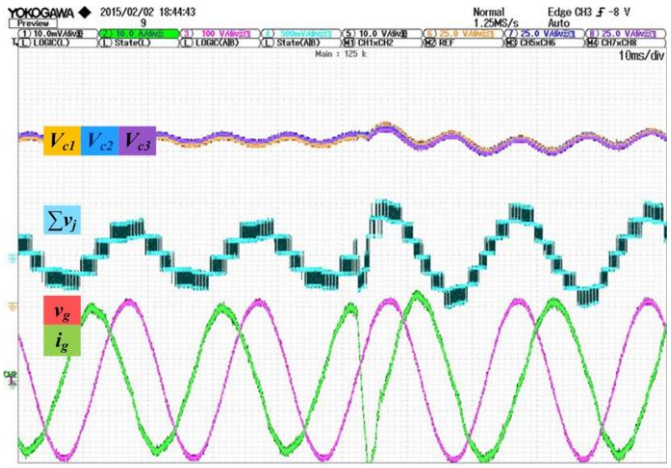

Fig. 19. Control system performance during sudden reactive power change with -25% decrease in *L*.

always remain in the linear region of the B-H curve of the inductor. The robustness of the d-q current controller to the parameter *L* was investigated in several references where it was shown that the controller remained robust to inaccuracy of *L* [32, 33]. Furthermore, minor deterioration in the performance of the current controller does not affect the rest of the control system because its dynamic is much faster than the rest of the controllers (as it is the inner control loop). To demonstrate the robustness of the proposed control system to the variations in *L* additional experimental tests in which the value of *L* was changed by ±25% are performed. As it can be seen from Figs. 18 and 19, the control system maintains good performance even with ±25% change in the value of *L*.

VII. Conclusions

In this paper a decoupled control system for a CHB multilevel converter-based STATCOM has been proposed. Two decoupling conditions which (i) eliminate the effect of the individual voltage controllers on the cluster voltage controller and the current controller and (ii) linearize the cluster voltage control loop have been derived. The first decoupling condition requires that the sum of the squares of the capacitor voltages in the cluster voltage controller is controlled to be constant and the second condition requires that the sum of the changes applied by the individual voltage controllers to the H-bridges output voltages is zero. Experimental results on a 7-level CHB based STATCOM demonstrated the effectiveness of the proposed decoupled control system in improving the transient responses. The proposed decoupled control system can also be applied to three-phase CHB multilevel converters which are basically composed of three identical single phase legs.

References

[1] F.Z. Peng; J.S Lai; J.W. McKeever; J. VanCoevering, "A multilevel voltage-source inverter with separate DC sources for static VAr generation,", *IEEE Transactions on Industry Applications*, vol.32, no.5, pp.1130-1138, Sep/Oct 1996

[2] J.S. Lai; F.Z. Peng, "Multilevel converters-a new breed of power converters, "*IEEE Transactions on Industry Applications*, vol.32, no.3, pp.509-517, May/Jun 1996

[3] E. Villanueva; P. Correa; J. Rodriguez; M. Pacas, "Control of a Single-Phase Cascaded H-Bridge Multilevel Inverter for Grid-Connected Photovoltaic Systems," *IEEE Transactions on Industrial Electronics*, vol.56, no.11, pp.4399-4406, Nov. 2009

[4] J. Chavarria; D. Biel; F. Guinjoan; C. Meza; J.J. Negroni, "Energy-Balance Control of PV Cascaded Multilevel Grid-Connected Inverters Under Level-Shifted and Phase-Shifted PWMs," *IEEE Transactions on Industrial Electronics*, vol.60, no.1, pp.98-111, Jan. 2013

[5] C. Cecati; F. Ciancetta; P. Siano, "A Multilevel Inverter for Photovoltaic Systems With Fuzzy Logic Control," *IEEE Transactions on Industrial Electronics*, vol.57, no.12, pp.4115-4125, Dec. 2010

[6] S. Du; J. Liu; J. Lin; Y. He, "A Novel DC Voltage Control Method for STATCOM Based on Hybrid Multilevel H-Bridge Converter," *IEEE Transactions on Power Electronics*, vol.28, no.1, pp.101-111, Jan. 2013

[7] R. Sternberger and D. Jovcic, "Analytical modelling of a square-wave controlled cascaded multilevel STATCOM," *IEEE Trans. Power Del.*, vol. 24, no. 4, pp. 2261–2269, Oct. 2009.

[8] H. Sepahvand; J. Liao; M. Ferdows.; K.A. Corzine, "Capacitor Voltage Regulation in Single-DC-Source Cascaded H-Bridge Multilevel Converters Using Phase-Shift Modulation," *IEEE Transactions on Industrial Electronics*, vol.60, no.9, pp.3619-3626, Sept. 2013

[9] B. Gultekin; M. Ermis, "Cascaded Multilevel Converter-Based Transmission STATCOM: System Design Methodology and Development of a 12 kV ±12 MVAr Power Stage," *IEEE Transactions on Power Electronics*, vol.28, no.11, pp.4930-4950, Nov. 2013

[10] T. Zhao; G. Wang; S. Bhattacharya; A.Q. Huang, "Voltage and Power Balance Control for a Cascaded H-Bridge Converter-Based Solid-State Transformer," *IEEE Transactions on Power Electronics*, vol.28, no.4, pp.1523-1532, April 2013

[11] L.K. Haw; M. S.A. Dahidah; H.A.F. Almurib, "SHE-PWM Cascaded Multilevel Inverter with Adjustable DC Voltage Levels Control for STATCOM Applications," , *IEEE Transactions on Power Electronics*, (Early Access)

[12] C. Townsend, T. Summers, and R. Betz, "Multi-goal heuristic model predictive control technique applied to a cascaded h-bridge statcom," *IEEE Transactions on Power Electronics.*, vol. 27, no. 3, pp. 1191–1200, 2012.

[13] C.D. Townsend; T.J. Summers; J. Vodden; Watson, A.J.; Betz, R.E.; Clare, J.C., "Optimization of Switching Losses and Capacitor Voltage Ripple Using Model Predictive Control of a Cascaded H-Bridge Multilevel StatCom," *IEEE Transactions on Power Electronics*, vol.28, no.7, pp.3077-3087, July 2013

[14] H. Iman-Eini; J. Schanen; S. Farhangi; J. Roudet, "A Modular Strategy for Control and Voltage Balancing of Cascaded H-Bridge Rectifiers," *IEEE Transactions on Power Electronics*, vol.23, no.5, pp.2428-2442, Sept. 2008

[15] M. Moosavi; G. Farivar; H. Iman-Eini; S.M. Shekarabi, "A Voltage Balancing Strategy With Extended Operating Region for Cascaded H-Bridge Converters," *IEEE Transactions on Power Electronics*, vol.29, no.9, pp.5044-5053, Sept. 2014

[16] J. Vodden; P. Wheeler; L.G. Franquelo; J.I. Leon; S. Vazquez, "One dimensional feed-forward modulation of a cascaded H-bridge multi-

level converter including capacitor balancing with reduced switching frequency," *Proceedings of the 14th European Conference on Power Electronics and Applications (EPE)*, ,pp.1-10, Aug. 2011

[17] J.A. Barrena; L. Marroyo; M.A. Rodriguez, J.R. Torrealday, "A Novel PWM Modulation Strategy for DC Voltage Balancing in Cascaded H-Bridge Multilevel Converters," *The International Conference on "Computer as a Tool EUROCON"*, pp.1450- 456, 9-12 Sept. 2007

[18] P. Karamanakos; K. Pavlou; S. Manias, "An Enumeration-Based Model Predictive Control Strategy for the Cascaded H-Bridge Multilevel Rectifier," *IEEE Transactions on Industrial Electronics*, vol.61, no.7, pp.3480-3489, July 2014

[19] M.B. de Alvarenga; J.A. Pomilio, "Voltage Balancing and Commutation Suppression in Symmetrical Cascade Multilevel Converters for Power Quality Applications," *IEEE Transactions on Industrial Electronics*, vol.61, no.11, pp.5996-6003, Nov. 2014

[20] L. Tarisciotti; P. Zanchetta; A. Watson; S. Bifaretti; J.C. Clare; P.W. Wheeler, "Active DC Voltage Balancing PWM Technique for High-Power Cascaded Multilevel Converters," *IEEE Transactions on Industrial Electronics*, vol.61, no.11, pp.6157-6167, Nov. 2014

[21] B.P. McGrath; D.G. Holmes; W.Y. Kong, "A Decentralized Controller Architecture for a Cascaded H-Bridge Multilevel Converter," *IEEE Transactions on Industrial Electronics*, vol.61, no.3, pp.1169-1178, March 2014

[22] A.D Aquila, M. Liserre, V.G Monopoli, P. Rotondo "Overview of PI-Based Solutions for the Control of DC Buses of a Single-Phase H-Bridge Multilevel Active Rectifier," *IEEE Transactions on Industry Applications*, vol.44, no.3, pp.857-866, May-june 2008.

[23] J.A. Barrena; L. Marroyo; M.A.R. Vidal; J.R.T. Apraiz, "Individual Voltage Balancing Strategy for PWM Cascaded H-Bridge Converter-Based STATCOM," *IEEE Transactions on Industrial Electronics*, vol.55, no.1, pp.21-29, Jan. 2008.

[24] Y. Liu; A.Q. Huang.; W. Song; S. Bhattacharya; G. Tan, "Small-Signal Model-Based Control Strategy for Balancing Individual DC Capacitor Voltages in Cascade Multilevel Inverter-Based STATCOM," *IEEE Transactions on Industrial Electronics*, vol.56, no.6, pp.2259-2269, June 2009.

[25] H. Akagi; S. Inoue; T. Yoshii, "Control and Performance of a Transformerless Cascade PWM STATCOM With Star Configuration," *IEEE Transactions on Industry Applications*, vol.43, no.4, pp.1041-1049, July-aug. 2007

[26] M. Zygmanowski; B. Grzesik; J. Michalak, "Power conditioning system with cascaded H-bridge multilevel converter DC-link voltage balancing method," *Power Proceedings of the 14th European Conference on Electronics and Applications (EPE)*, pp.1-10, Aug. 30 2011-Sept. 1 2011

[27] A.A. Valdez-Fernandez; P.R. Martinez-Rodriguez; G. Escobar; C.A. Limones-Pozos; J.M. Sosa, "A Model-Based Controller for the Cascade H-Bridge Multilevel Converter Used as a Shunt Active Filter," *IEEE Transactions on Industrial Electronics*, vol.60, no.11, pp.5019-5028, Nov. 2013

[28] X. She; A.Q. Huang; T. Zhao; G. Wang, "Coupling Effect Reduction of a Voltage-Balancing Controller in Single-Phase Cascaded Multilevel Converters," *IEEE Transactions on Power Electronics*, vol.27, no.8, pp.3530-3543, Aug. 2012

[29] Z. Liu; B. Liu; S. Duan; Y. Kang, "A Novel DC Capacitor Voltage Balance Control Method for Cascade Multilevel STATCOM," *IEEE Transactions on Power Electronics*, vol.27, no.1, pp.14-27, Jan. 2012

[30] J.F. Sultani, "Modelling, Design and Implementation of d-q Control in Single-Phase Grid-Connected Inverters for Photovoltaic Systems Used in Domestic Dwellings" Ph.D. dissertation, Faculty of Technology, De Montfort Univ, Leicester, UK, 2013.

[31] S. Kouro; P. Lezana; M. Angulo; J. Rodriguez, "Multicarrier PWM With DC-Link Ripple Feedforward Compensation for Multilevel Inverters," *IEEE Transactions on Power Electronics*, vol.23, no.1, pp.52-59, Jan. 2008

[32] M. Monfared; S. Golestan; J.M. Guerrero, "Analysis, Design, and Experimental Verification of a Synchronous Reference Frame Voltage Control for Single-Phase Inverters," *IEEE Transactions on Industrial Electronics*, vol.61, no.1, pp.258-269, Jan. 2014;

[33] B. Bahrani , A. Rufer , S. Kenzelmann and L. Lopes "Vector control of single-phase voltage source converters based on fictive axis emulation", *IEEE Trans. Ind. Appl.*, vol. 47, no. 2, pp.831 -840 2011